PROCEEDINGS OF THE ROYAL SOCIETY A

rspa.royalsocietypublishing.org

Research

Article submitted to journal

Subject Areas:
Atmospheric Science

Keywords:
cloud brightening, aerosols, cloud-drops, albedo, geoengineering

Author for correspondence:
Paul James Connolly
e-mail: p.connolly@man.ac.uk

Royal Society Publishing
Informing the science of the future

Factors determining the most efficient spray distribution for marine cloud brightening

P. J. Connolly[1], G. B. McFiggans[1] and R. Wood[2]

[1]School of Earth, Atmospheric and Environmental Science, University of Manchester, Manchester, UK
[2]Department of Atmospheric Sciences, University of Washington, Seattle, Washington, USA

We investigate the sensitivity of marine cloud brightening to the properties of the added salt particle distribution using a cloud parcel model, with an aim to address the question of, "what is the most efficient particle size distribution, that will produce a desired cooling effect?". Our findings suggest that this question depends on the spray generation method. For both the *supercritical fluid* and the *Taylor cone-jet* methods of spray generation salt particles within the median dry diameter range $D_m = 30$ to 100 nm, that have realistic size distributions, are the are the most effective range of sizes. This is also true for the *Rayleigh jet* method with median dry diameters between 30 and 100 nm being the most effective for the required change in albedo. The *Rayleigh-jet* method is also the most energy efficient when compared to the *supercritical fluid* and *Taylor cone-jet* method. We also find that care needs to be taken when using droplet activation parameterisations: for the concentrations considered Aitken particles do not result in a decrease in the total albedo, as was found in a recent study, and such findings are likely a result of the parameterisations in ability to simulate the effect of swollen aerosol. Our findings suggest that persistent hazes may play a role in controlling the albedo rather than just the activated cloud drops, which is an effect that the parameterisation methods do not easily take account of.

1. Introduction

Marine cloud brightening is a proposed method to reduce the effects of global warming due to rising CO_2 levels (*Latham*, 1990, 2002). For a recent review of latest developments on this topic see *Latham et al.* (2012).

The method involves using large numbers of ships to spray nebulised sea water into rising air below a marine boundary layer cloud. The resulting increased cloud condensation nucleus (CCN) concentrations mean that cloud droplet concentrations are increased, which has been hypothesized to result in clouds that are more reflective (*Twomey*, 1977) and longer lasting (*Albrecht*, 1989).

Research into this area of geoengineering has asked the question, *'what is the most efficient spray size?'*, which would result in a significant change to the cloud albedo (*Alterskjaer and Kristjánsson*, 2013; *Bower et al.*, 2006; *Latham et al.*, 2012), without specifying what quantity the efficiency was being evaluated against. These former studies investigated the impact, on the change in cloud albedo, of adding sea spray of different sizes and at different particle *number concentrations*. However, central to optimising the spray properties is the quantity we are trying to optimise with respect to. An obvious quantity to attempt to optimise is the amount of energy / power used to spray the aerosol into the atmosphere, which is the quantity we will focus on herein.

At the time of writing there are three main techniques (see *Neukermans et al.*, 2013) of generating the sea spray that are possible candidates to consider in such a large-scale application. For an overview of these methods see Appendix A and references therein. Analysis of each of these spray techniques reveals that the power (electrical, mechanical or heat) that the spray techniques consume depends on either the flow rate of sea spray into the atmosphere, Q (in the case of the super critical fluid and Taylor cone-jet spray techniques), or depends on the product of flow rate and reciprocal of the aerosol size, $\left(\frac{a}{D_m}+b\right)Q$ (in the case of the Rayleigh jet instability method). Hence, in our paper we address the question of what are the optimal spray particle parameters for: (i) a given mass of sea water sprayed, Q; and (ii) for the parameter $\chi=\left(\frac{a}{D_m}+b\right)Q$, where Q is the mass of sea water sprayed and D_m is the median dry diameter of the injected aerosol particles. We show in the appendices that these two parameters should approximately scale with the amount of energy that either of the proposed spray methods use (see Appendices for details).

We also address the use of *physically-based parameterisation schemes* for determining the optimal spray parameters. Our aim here is to investigate in detail an effect shown by *Alterskjaer and Kristjánsson* (2013), where very small injected aerosol particles suppressed the cloud albedo, rather than enhanced it. Recently, *Alterskjaer and Kristjánsson* investigated the effect of injecting sea spray into marine boundary layer clouds in a global model. A physically-based parameterisation was used to determine how many cloud droplets would form on a combination of background aerosol and sea spray aerosol. Their results indicated that injecting small Aitken mode particles (in the range $30 \leq D_p \leq 50$ nm) could result in a reduction rather than an increase in cloud albedo. This is counter intuitive since one would normally expect that the majority of Aitken mode particles would remain interstitial and not significantly affect the reflective properties of the cloud, due to the effect of the high curvature of their surface on the equilibrium vapour pressure of water. Such an effect was not seen in earlier studies by *Bower et al.* (2006); *Latham et al.* (2012). Hence in this paper we will also attempt to reconcile the differences put forward by the aforementioned studies.

2. Methods

We make use of the same models described by *Simpson et al.* (2014). They are explained briefly here.

(a) The explicit model

The model used is the Aerosol-Cloud and Precipitation Interactions Model (ACPIM), a cloud model with bin-microphysics which was developed at The University of Manchester (*Connolly et al.*, 2012). The aerosol size distribution is input as several lognormally distributed 'modes', which are discretised into size bins, each mode requiring the particle number concentration, N, the median particle diameter, D_m, and the geometric standard deviation, $\ln\sigma_g$. In this study it is configured so that each mode of the aerosol particle size distribution is split into 200 bins with a minimum size of 5 nm. To best resolve the splitting of the aerosol population upon activation into cloud drops the aerosol bin-widths are configured so that they each contain the same number concentration of particles. The relevant calculation of the albedo is described in *Latham et al.* (Section 4a 2012); however, the difference in this work is that we now use Mie theory to explicitly calculate the extinction efficiency of the aerosols and drops as a function of their size, rather than assume that the extinction efficiency is equal to 2. It is important to use the extinction efficiency calculated from Mie Theory in situations where large quantities of small aerosol particles are added (which have a large total projected area, but almost negligible extinction efficiency). The optical depth was calculated by integrating the extinction in the vertical as in *Latham et al.* (Eq. 4.3 2012).

(b) The parameterisations

To try and reconcile the results put forward by *Alterskjaer and Kristjánsson* (2013) with the results presented by *Latham et al.* (2012) we have used two droplet activation schemes to compare to the parcel model. The schemes used are (i) the *Abdul-Razzak et al.* (1998) scheme, which was used in the *Alterskjaer and Kristjánsson* study and (ii) the *Fountoukis and Nenes* (2005) scheme. Both are quite similar in that they take T, P and aerosol properties as an input and output the peak supersaturation and number of activated drops; however, the first scheme uses an approximate analytical solution to find the peak in supersaturation at cloud base, whereas the second method uses an iterative method to find the maximum. The aerosol size distributions are input as lognormally distributed 'modes', but are not discretised into size bins, like in the explicit model above.

Mie theory could not be used to calculate the extinction for the parameterisation methods as there is no information on the size of the unactivated aerosol particles as they swell due to an increase in humidity. Instead, for these parameterisation methods, we assume that the extinction is dominated by the cloud drops and that they have an extinction efficiency of 2. The albedo was calculated from the activated droplet number concentration by assuming that the liquid water mixing ratio increased linearly with height, $q_l = az$, where z is height above cloud base. A cloud depth of 160 m was used so that the cloud top liquid water mixing ratio was 0.27 g kg^{-1}, which is typical for marine stratocumulus and consistent with the explicit model (Section (a)). These parameters were also chosen so that the cloud albedo, $A_c \sim 0.4$, in the simulation with no added salt particles (consistent with *Bender et al.*, 2011).
In this case, assuming all particles are the same size, the extinction is:

$$\beta(z) = \left(\frac{6a}{\rho\pi}\right)^{2/3} \frac{\pi N^{1/3}}{2} z^{2/3} \tag{2.1}$$

and the optical depth of the cloud is (the vertical integral of Equation 2.1):

$$\tau = \left(\frac{6a}{\rho\pi}\right)^{2/3} \frac{\pi N^{1/3}}{2} \frac{3}{5} z_c^{5/3} \tag{2.2}$$

where z_c is the cloud thickness, N is the number mixing ratio of cloud drops and $a = 1.67 \times 10^{-6}$ is a constant. A relationship from *Seinfeld and Pandis* (2006) is used to relate the diurnal mean albedo of a cloud, A_c, to the optical depth via:

$$A_c \cong \frac{\tau}{\tau + 7.7} \tag{2.3}$$

(c) Model set-up

The aerosol size distributions measured during a recent field campaign that sampled marine stratocumulus clouds off the Chilean coast (*Allen et al.*, 2011) were used as a basis for the background aerosol size distribution in this study (see Table 1). We used the 'remote' region away

Table 1. Background aerosol lognormal fit parameters for the 'remote' region in VOCALS (see *Allen et al.*, 2011). *Allen et al.* (2011) define the remote region as that west of 80°W.

	Mode 1	Mode 2	Mode 3
$N(m^{-3})$	46.64×10^6	153.42×10^6	166.77×10^6
$\ln \sigma$	0.348	0.354	0.465
$D_m(nm)$	18	39	154

from the coast, which used *in-situ* measurements of aerosol particles west of 80°W along 20°S. This region is over the South East Pacific ocean, away from the near-coastal polluted regions, and is frequently considered as being suitable for marine cloud brightening in global modelling studies (e.g. *Alterskjaer and Kristjánsson*, 2013; *Jones et al.*, 2010).

We performed several sensitivity studies with the model for an updraft speed of 0.3 m s^{-1} and with the injected (salt mode) aerosol having $\ln \sigma = 0.25$ (narrow) and 0.5 (broad) lognormal distribution parameters. We also varied the median diameter, D_m, of the salt mode using values of 20, 30, 45, 95, 200, 500, 1000 nm. The total NaCl mass mixing ratio, q_{salt}, defined as the total mass of NaCl per unit mass of air, was varied by changing the particle number concentration of the lognormal input distribution, N. The total NaCl mass mixing ratio, q_{salt}, was varied between 10^{-14} to 10^{-4} kg kg^{-1} (this equates to 10^{-5} to 10^{5} μg kg^{-1}), each subsequent run having mass mixing ratios that were 10 times the previous run.

3. Results

(a) Most efficient sizes / spray technique

The flow rate of water into the atmosphere, Q, depends on what fraction of the earth the scheme is applied to and the *mixing ratio of salt*, q_{salt}, that is required in that region (Appendix B). Since the energy used by the sprayers is either proportional to Q (supercritical fluid and Taylor cones-jets) or $\left(\frac{a}{D_m} + b\right) Q$ (Rayleigh-jets), and Q is proportional to q_{salt}, we choose to plot our results as a function of either *salt mass mixing ratio* or the *salt mass mixing ratio* multiplied by $\left(\frac{0.45}{D_m} + 3.2 \times 10^6\right)$ (see Equation A 8). This enables an assessment of the most efficient spray distribution for the two different spray techniques by assigning a value of albedo that is ~ 0.05 greater than the baseline case and reading off the graph what the corresponding x-axis value is. The x-value is then multiplied by a constant to scale up to total power required, which depends on spray technique.

Figure 1 shows results from the ACPIM bin model for an updraft speed of 0.3 m s^{-1} and a $\ln \sigma = 0.5$. Figure 1a shows the number of cloud drops that are formed as a function of q_{salt} for different values of median dry diameter of the NaCl particles, D_m. We have plotted the response of the cloud / aerosol particles in different ways. Panels b and c show how the albedo of the aerosol and cloud particles changes for different values of q_{salt} and NaCl particle concentrations; panels d and e show similar plots but just for the cloud drops (i.e. those particles that grow into cloud drops and do not remain as 'interstitial' aerosol particles); and panels f and g show similar plots but just for the interstitial (non-cloud) aerosol particles. Generally it can be seen that at high values of q_{salt} the albedo response is dominated by the interstitial aerosol particles (i.e. the albedo due to the cloud reduces rapidly for $q_{salt} > 10^{-6}$, but for aerosols it increases to values close to unity), whereas at low values of q_{salt} it is dominated by the cloud particles (i.e. the albedo due to aerosols is almost zero for $q_{salt} < 10^{-10}$, but for the cloud it is ~ 0.4).

It is interesting to note that for NaCl mixing ratios that are between 10^{-10} and $\sim 10^{-7}$ the particle sizes that are most effective at changing the albedo of the cloud are particle median dry sizes that are in the range $30 \leq D_p \leq 100$ nm (see Figure 1, panel b). This suggests that using these particle sizes would be the most efficient way (in terms of least energy consumed) of changing the cloud albedo when using either the *supercritical fluid* or the *Taylor cone-jet* methods of spray generation. However, in terms of number of particles added, it can be seen that the larger particles are the most effective at changing the albedo (Figure 1, panel c), which is consistent with previous findings. We also see that particle sizes of 30 nm produce the largest cloud drop concentrations (Figure 1a) and that the dependence of drop concentration on *salt mixing ratios* is monotonic for *mixing ratios* less than $\sim 10^{-8}$ to 10^{-7}.

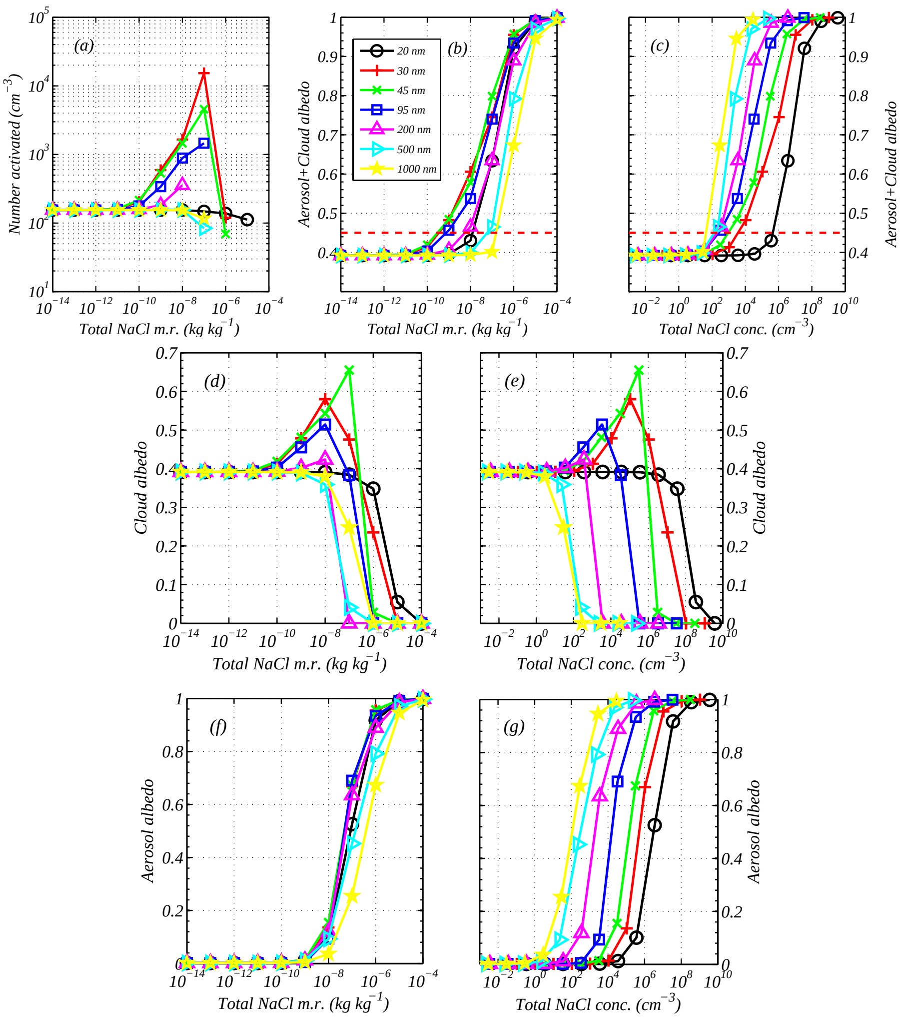

Figure 1. Shows the results from using the ACPIM bin model for different median diameters of the injected aerosol ($\ln\sigma = 0.5$, $w = 0.3$ m s^{-1}). (a) Shows the number of activated drops vs the mass mixing ratio of NaCl particles; (b) shows the total albedo vs the mass mixing ratio of NaCl particles; (c) shows the total albedo vs the number concentration of added NaCl particles. Red dashed line is the approximate required value of albedo for geoengineered clouds. (d-e) same as panels b and c, but just for the cloud particles; (f-g) same as panels b and c, but just for the unactivated aerosol particles

Figure 2 shows the same data from Figure 1 except that instead of plotting the albedo as a function of total NaCl mixing ratio we have plotted the albedo against a variable, $\chi = \left(\frac{0.45}{D_m} + 3.2\times 10^6\right) q_{salt}$. The reason we have chosen to plot against this variable is because it should be proportional to the energy used by the *Rayleigh-jet* method (see Equation A 8, Section A). Figure 2 shows that, for values of χ between 10^{-3} and 10^{-1}, particle median diameters between 30 to 100 nm are the most effective at changing the albedo. At values of χ greater than 10^{-1} the 30 nm particles become less efficient than the 45 and 100 nm particles. 45 and 100 nm particles are the most efficient at all sizes.

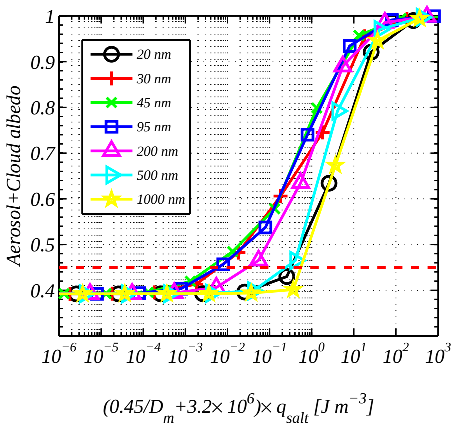

Figure 2. Shows the results from using the ACPIM bin model for different median diameters of the injected aerosol ($\ln\sigma = 0.5$, $w = 0.3$ m s^{-1}). Data are plotted as the albedo vs a variable $\chi = \left(\frac{0.45}{D_m} + 3.2\times 10^6\right) q_{salt}$ (see Section 1 for details). Red dashed line is the approximate required value of albedo of geoengineered clouds.

(b) Parameterisation methods

Figure 3 shows how the different parameterisations (see Section 2(b)) behave for an updraft speed of 0.3 m s^{-1} and a $\ln\sigma = 0.5$ and can be compared to the bin model calculations in Figure 1(a-c). It is clearly shown in Figure 3, panels (b-c) that, for all but the smallest median diameter particles ($D_m = 20$ nm), the *Abdul-Razzak et al.* scheme shows a sharp 'drop off' in the predicted albedo as the mixing ratio of NaCl particles (or number concentration increases). We suspect that this is the region in the aerosol size distribution parameter space where *Alterskjaer and Kristjánsson* (2013) noted a positive radiative effect when adding Aitken particles. This is not evident in the *Fountoukis and Nenes* scheme (panels e-f). In general though the albedo changes due to adding salt particles are significantly underestimated by both schemes, which is due to the fact that neither of the parameterisation methods treat un-activated aerosol in the calculations of albedo. It is evident that both of the parameterisation schemes were not designed for the range of inputs that are relevant for geoengineering applications, in which there can be a large quantity of un-activated aerosol particles and as a result they perform poorly when compared to the parcel model (Figure 1(a-c)). For the *Abdul-Razzak et al.* scheme the number of activated particles and hence cloud albedo reduces as q_{salt} is increased (Figure 3(a a,b). This behaviour is qualitatively consistent with the cloud albedo from the parcel model (Figure 1d); however, the parameterisation scheme does not take into account the significance of the large quantities of unactivated swollen aerosol particles.

(c) Effect of narrowing the spray distribution

It should be noted that the width parameter, $\ln\sigma_g$, of the injected aerosol also influences the choice of the most efficient spray distribution. To demonstrate the role that $\ln\sigma$ plays we performed addition bin model runs, varying $\ln\sigma$ from 0.025 (which is close to values the *Rayleigh-jet* technique may achieve, Appendix (a)) to 0.5 (which is what the *supercritical fluid* technique can achieve, Appendix (c)). We did these calculations for a constant mass mixing ratio of salt particles

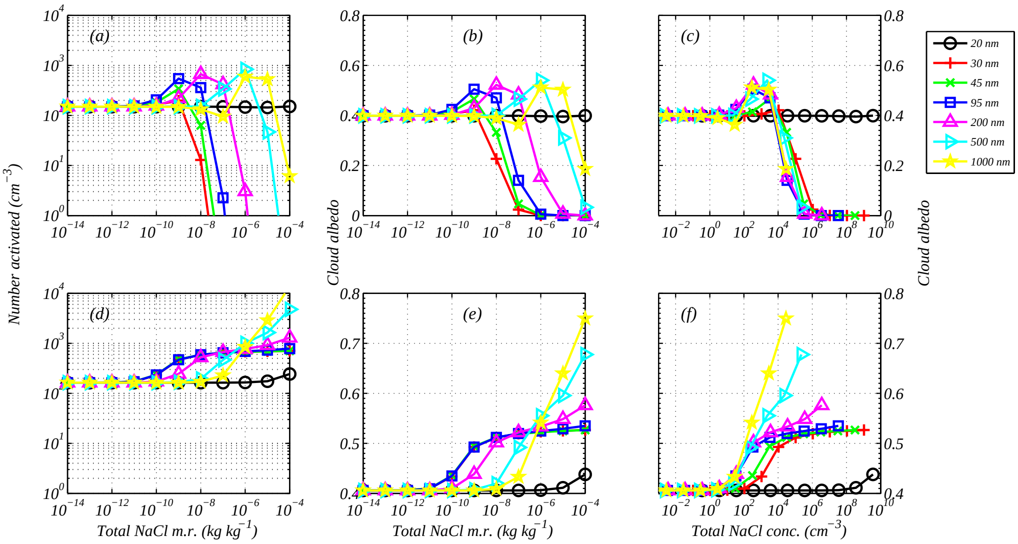

Figure 3. Shows results from different cloud droplet activation parameterisations. (a-c) is the *Abdul-Razzak et al.* scheme; (d-f) is the *Fountoukis and Nenes* scheme. (a / d) Shows the number of activated drops vs the mass mixing ratio of NaCl particles; (b / e) shows the albedo vs the mass mixing ratio of NaCl particles; (c / f) shows the albedo vs the number concentration of added NaCl particles.

equal to 10^{-8}. The results of these calculations are shown in Figure 4 and confirm that larger aerosol particle median diameters can result in a more effective increase in the albedo as the width of the distribution decreases; however, it is evident that, even for the most narrow distribution, the most efficient dry salt particle median diameters are still ~ 100 nm in diameter.

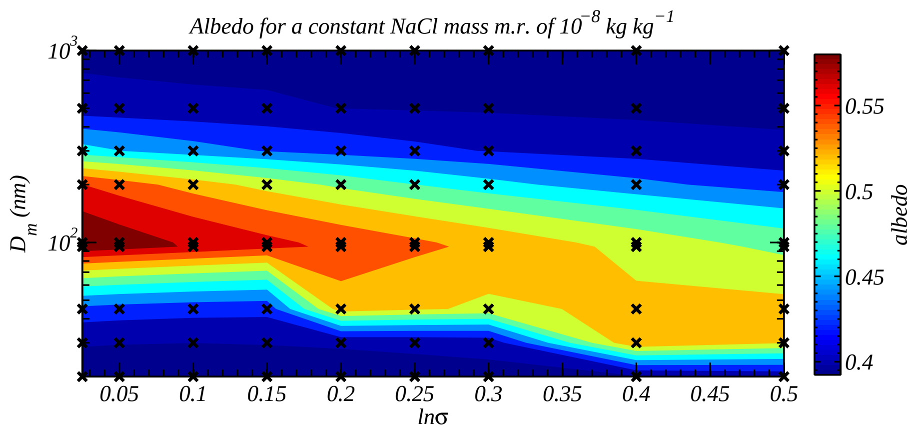

Figure 4. Shows calculations of the albedo for a constant NaCl mass mixing ratio of 1×10^{-8} kg kg^{-1} as a function of $\ln \sigma$ and D_m. This shows that for a narrow distribution the most efficient size is ~ 100 nm, whereas for the broadest distributions the most efficient size is ~ 30 nm.

4. Discussion

(a) Optimal spray parameters for each technique

Previous studies of marine cloud brightening have investigated the spray parameters that will be most effective for changing the albedo of the cloud. However, these studies have not considered the spray parameters that are most efficient for a given energy expenditure.

In determining the most efficient spray particle size for marine cloud brightening we have considered the two main methods of spray generation: the *supercritical fluid* method and the *spray-jet* method, which can be further subdivided into *Rayleigh instability-jets* or *Taylor cone-jets*. Our results suggest that the spray parameters that are the most efficient for the marine cloud brightening scheme depend on the spray technique used and the amount that the cloud albedo is to be changed by. For the all three methods dry particle median diameters in the range $30 \leq D_m \leq 100$ nm were the most effective with respect to the power consumption. This suggests that overall the most efficient sizes to aim for are around ~ 100 nm median diameter, which equates to the volume of an ~ 80 nm sided cube if the salt particles are assumed to be cubes.

The range of aerosol spray parameters investigated are consistent with those achieved by *Cooper et al.* (2013); however, the *Rayleigh instability-jet* method may be capable of producing narrower distributions, which would increase the size of the most efficient salt particles (see Figure 4). Nevertheless, this still implies median dry diameters of approximately 100 nm or so would be the most efficient.

Offline calculations using physically-based parameterisations of cloud activation have been used to understand the implementation of the marine cloud brightening scheme in large-scale models. Our results suggest that these parameterisations do not perform well within the parameter space relevant to marine cloud brightening. The *Abdul-Razzak et al.* (1998) scheme in particular predicts that large concentrations of Aitken particles lead to a significant reduction in the albedo, which is inconsistent with the parcel model results, mainly because it does not take in to account the swelling of unactivated aerosol particles at humidities close to water saturation. Although the *Fountoukis and Nenes* (2005) scheme was generally consistent and qualitatively similar to the parcel model it also did not quantitatively reproduce the correct range of results, both in terms of number of cloud drops and in terms of albedo.

Alterskjaer and Kristjánsson (2013) used the *Abdul-Razzak et al.* (1998) scheme within the NorESM model to investigate the marine cloud brightening scheme and arrived at the conclusion that the sign of radiative forcing was dependent on both particle size and the mass injected. They found that injecting accumulation mode particles had the desired negative radiative effect, but that injecting large quantities of Aitken mode particles resulted in positive radiative forcing. Such a finding is consistent with Figure 3, which highlights that the *Abdul-Razzak et al.* (1998) scheme does not perform well in this regime.

(b) Energy requirements

We now turn to the question of energy requirements for the different spray systems. *Latham et al.* (2008, page 3970) argue that, in order to offset the effects of rising levels of CO_2, the marine cloud brightening scheme needs to provide a negative radiative forcing of $\Delta F \sim -4$ W m^{-2} of the Earth's total $F = 340$ W m^{-2} average irradiance. *Latham et al.* (2008, Equations 3.1, 3.2 and 3.3) provide arguments to link the required forcing to a change in cloud albedo. Assuming that the clouds that are to be brightened cover 20 % of the Earth's surface the result (from *Latham et al.*, 2008, Equation 3.3) is that the change in cloud albedo has to equal:

$$\Delta A_c = -\frac{\Delta F}{340 \times 0.20} \tag{4.1}$$

which for $\Delta F = -4$ W m^{-2} yields $\Delta A_c \cong 0.06$; hence, the aim would be to change the albedo of marine stratocumulus clouds by an average of $+0.06$.

If we consider the Rayleigh-jet method we may insert Equation A 11 into Equation A 8 to obtain the power required by the sprayers in terms of the parameter, $\chi = \left(\frac{0.45}{D_m} + 3.2 \times 10^6\right) q_{salt}$:

$$P \cong \chi \left(\frac{AH}{S\tau}\right) \tag{4.2}$$

Figure 2 shows that the parameter, χ (the value of the x-axis), that achieves the required change in albedo for $30 \leq D_m \leq 100$ nm is $\sim 3 \times 10^{-3}$, so substituting this and other variables into Equation 4.2 yields a total power for the Rayleigh jet method of ~ 30 MW, which sounds reasonable for total energy consumed.

For the Taylor cone-jet method we may apply Equation A 12, which requires the total flow of water as input. Figure 1(b) shows that an NaCl mixing ratio of $\sim 0.5 \times 10^{-9}$ yields the required change in albedo using dry salt particle median diameters of $30 \leq D_m \leq 95$ nm, which if substituted into Equation A 11 yields the volume flow rate of sea water to be $Q \sim 5.5$ m^3 s^{-1}. We then estimate the total power required by this technique by substituting $Q = 5.5$ m^3 s^{-1} into Equation A 12, which yields a required power of $\sim 6.1 \times 10^3$ MW. Although the power consumption is still high with this method it is 1000 times less energy intensive than the current global power generation.

Let us now consider the supercritical flow spray technique. The NaCl mixing ratio of $\sim 0.5 \times 10^{-9}$ still holds for this technique and so $Q = 5.5$ m^3 s^{-1} is substituted into Equation A 15, which yields a required power of $\sim 2 \times 10^4$ MW; hence, this method is the most expensive in terms of power consumed by the sprayers.

5. Conclusions

Parcel model results:

- In terms of total mass of salt added the most efficient size to seed with is ~100 nm median diameter particles in general. However, for the supercritical fluid spray system it may be just as efficient to seed using particles with a dry median diameter as small as 30 nm.
- These parcel model results are not in agreement with the recent paper by *Alterskjaer and Kristjánsson* (2013), who found a negative response to the albedo when adding Aitken particles. This study used a parameterised model of activation to determine number of cloud drops (*Abdul-Razzak and Ghan*, 2000; *Abdul-Razzak et al.*, 1998).

Parameterisation results:

- We used two parameterisation methods to determine the cloud droplet number concentration for the same conditions as those simulated in the parcel model. They were (i) the *Abdul-Razzak et al.* (1998) scheme for lognormal aerosol distributions and (ii) the *Fountoukis and Nenes* (2005) scheme, which is also for lognormal aerosol distributions.
- Neither scheme reproduced the dynamical parcel model with high accuracy. In all cases the *Abdul-Razzak et al.* scheme resulted in a negative response of the cloud droplet number concentration as the total mass of aerosol increased past a threshold that depended on the size of the mode, whereas the *Fountoukis and Nenes* (2005) scheme did not reproduce a negative response. It appears that the reason the parameterisation methods do not well represent the parcel model results is that they do not consider the effect of swollen, unactivated aerosol particles on the albedo, which is a significant effect.
- The limitations of the physically-based parameterisations should be borne in mind when using them to study aerosol-cloud interactions within large-scale models.

Other:

- There are many other factors that determine what the most efficient spray distribution is. Here we have merely focussed on what we expect the most efficient spray parameters are for a given energy cost. However, factors such as energy availability; maintenance costs; engineering the apparatus to rapidly nebulize the sea spray; and factors that affect the transport of the spray into cloud base, such as the effect of latent cooling on the buoyancy of the air may all play an important role.
- Our simple calculations of energy usage suggest that the Rayleigh-jet method is the least energy intensive, followed by the Taylor cone-jet method and then the supercritical fluid method.
- Finally, in order to decide whether such a scheme would be beneficial, a thorough cost-benefit analysis is required.

A. Spray methods

(a) Jet-instability

Firstly, there is the technique that makes use of the instability of jets, which was analysed in detail by Lord Rayleigh (*Rayleigh*, 1878) and is the method proposed by *Salter et al.* (2008, page 3997). In such a technique the water jet breaks up into water drops that have a diameter equal to 1.89 times the diameter of the initial cylindrical jet. We now investigate the power requirements for spraying using this kind of jet.

The relationship between pressure drop across a nozzle, Δp, and flow through it, Q_s, is sought. We can interpret the pressure drop across the nozzle to be due to: (i) providing the high kinetic energy required for the jet, Δp_{KE}; (ii) capillary pressure due to surface tension, Δp_{ST}; (iii) viscous flow through the tube, Δp_{vis}:

$$\Delta p = \Delta p_{KE} + \Delta p_{ST} + \Delta p_{vis} \tag{A 1}$$

The pressure drop due to providing kinetic energy to the drops is

$$\Delta p_{KE} = \frac{\rho w}{2} v^2 \tag{A 2}$$

and it is argued that $v = 80$ m s^{-1} is an ideal flow speed to aim for to achieve good drop break-up, which gives $\Delta p_{KE} = 3.2 \times 10^6$ Pa.
For the capillary pressure we utilise the Young-Laplace equation:

$$\Delta p_{ST} = \frac{4\sigma}{D_n} \tag{A 3}$$

where $\sigma = 0.072$ N m^{-1} (at -20°C) and D_n is the diameter of the end of the nozzle, which results in $\Delta p_{ST} \cong \frac{0.3}{D_n}$ (units are Pa if D_n is in metres).
Hagen-Poiseuille flow describes the pressure drop, ΔP_{vis}, in a fluid of viscosity μ that is flowing down a pipe of length L, diameter d_p. The equation describing the pressure drop is

$$\Delta p_{vis} = \frac{128\mu L Q_s}{\pi d_p^4} \tag{A 4}$$

where Q_s is the flow rate down a single nozzle and L is the length of the pipe.

The viscous pressure drop across a tapered nozzle, as in (*Salter et al.*, 2014, their figure 4) can be described by integrating contributions of to the pressure drop due to elements of the nozzle that obey Hagen-Poiseuille flow. The angle of the taper is 35.26° because it is etched from a crystal. The length of the whole nozzle is $2.4\,\mu$m and the diameter at the un-tapered end is $1.5\,\mu$m. The diameter of the exit hole of the nozzle, D_n, is considered to be variable. This leads to:

$$\Delta p_{vis} = \frac{128\mu Q_s}{\pi} \int_0^{2.4\,\mu m} \frac{1}{d_p\left(x\right)^4} dx \tag{A 5}$$

where $d_p\left(x\right)$ is a function describing the diameter of the nozzle along the length of the nozzle, x. In order to evaluate the integral we have to split it into two terms (one describing the $1.5\,\mu$m pipe and another describing the taper). A good approximation to this integral is:

$$\Delta p_{vis} = \frac{128\mu Q_s}{\pi} \left[\frac{1}{4.24} \frac{1}{D_n^3}\right] \tag{A 6}$$

With $Q_s = \frac{\pi}{4} D_n^2 \times v$ and $v = 80$ m s^{-1} we find that $\Delta p_{vis} \cong \frac{0.60}{D_n}$ (units are Pa if D_n is in metres).

The power required to pump the liquid through the system is the pressure drop multiplied by the volume flow rate. Hence we may write down an equation that describes the power (watts) needed for a given flow rate, Q (m^3 s^{-1}):

$$P_w = \left(\frac{0.90}{D_n} + 3.2 \times 10^6\right) Q \tag{A 7}$$

$$\cong \left(\frac{0.45}{D_m} + 3.2 \times 10^6\right) Q \tag{A 8}$$

the second line is derived from the fact that the drop diameter is ~ 2 times the nozzle diameter and the drop diameter is ~ 4 times the dry aerosol diameter, D_m, so $D_n \cong 2D_m$.

(b) Taylor Cone-jets

Here we provide arguments for the application of Hagen-Poisseuille flow to the case of Taylor Cone-jets and show that it is consistent with measurements by (*Neukermans et al.*, 2013).

The Taylor Cone-jet method uses an untapered nozzle and does not require the pump to provide drops with a high kinetic energy, since an electric field provides the kinetic energy instead. For an untapered nozzle the power is therefore due to overcoming pressure drop due to viscosity and surface tension:

$$P_w = \left(\frac{128\mu L Q_s}{\pi D_n^4} + \frac{4\sigma}{D_n}\right) Q \tag{A 9}$$

Application of an electric potential to liquid-filled capillary tubes results in an electrospray (see *Taylor*, 1964). *Cooper et al.* (2013, page 87) studied the electrospray technique using 16 μm diameter capillaries to generate ~ 100 nm salt cubes from sea water. For a salinity of 35 kg m^{-3}, 100 nm salt cubes implies that the sea water drop diameters were ~ 750 nm and likely had a geometric standard deviation of $\ln \sigma_g = 0.45$. The volume of water in a drop distribution that is lognormally distributed can be calculated via the third moment of a lognormal distribution (`http://en.wikipedia.org/wiki/Log-normal_distribution#Arithmetic_moments`):

$$Q = n\frac{\pi}{6} \times \exp\left(3\ln\left[d\right] + 4.5\ln^2\sigma_g\right) \tag{A 10}$$

where $d = 750 \times 10^{-9}$ m is the drop diameter, $n = 1 \times 10^9$ s^{-1} is the number of particles sprayed per second by a single electrospray and $\ln \sigma_g = 0.45$. These values yield $Q \sim 5.6 \times 10^{-10}$ m^3 s^{-1}

A single electrospray generates $n = 1 \times 10^9$ particles per second (*Neukermans et al.*, 2013, page 513). The mechanical power, P_m, required to generate the spray from a single nozzle can therefore be estimated using Equation A 9, assuming $L = 1 \times 10^{-3}$ m; $d = 16 \times 10^{-6}$ m (the diameter of the capillary), with $Q \sim 5.6 \times 10^{-10}$ m^3 s^{-1} provided by Equation A 10. *Neukermans et al.* (2013) then argue that the mechanical power required for a single nozzle should be scaled up by 1×10^8 for a single application-sized unit with 1×10^8 nozzles, each with $Q_s = 5.6 \times 10^{-10}$ m^3 s^{-1}, and that such a unit would use 20 kW of mechanical power. Our calculation assuming Hagen-Poisseuille flow is consistent this and yields 20.5 kW.

Energy is also required to apply an electrical potential to the nozzle, since a current results by the movement of the charged drops Cooper *et al.* (2013, page 85), which they argue dominates over the mechanical power requirement. Neukermans *et al.* (2013, page 514) report that the electrical power requirements are 130 kW for a potential of 3.4 kW and current of $1.8\,\mu$A. This is for a volume flow rate of 0.33 L s^{-1}, which is a conversion factor of $\frac{130\times10^3}{0.33\times10^{-3}} \cong 4\times10^8$ W m^{-3}. It is to be noted that this is less than the theoretical electrical power required $V\times I = 6.12\times10^{-3}$ watts per nozzle, or 612 kW for the whole system. However, Cooper *et al.* (2013, page 95) provide estimates of 4 mW per nozzle, with a 3 kV potential and $1.33\,\mu$A current which are consistent with the theoretical calculation. The 4 mW per nozzle figure was for a 3.3×10^{-12} m^3 s^{-1} flow rate, which is a conversion factor of 1.2×10^9 W m^{-3}.

Hence using the values that are consistent with theory, the total power required for this technique is:

$$P_t = \left(\frac{128\mu L Q_s}{\pi D_n^4} + \frac{4\sigma}{D_n} + 1.2\times10^9\right) Q \quad \text{(A 11)}$$

$$\cong 1.2\times10^9 Q \quad \text{(A 12)}$$

The first two terms have been neglected as they are vastly out-weighed by the 3rd term.

(c) Supercritical flow spray

Finally, there is the technique of heating up the sea water to its supercritical point and then pumping the supercritical fluid through a nozzle (Neukermans *et al.*, 2013). The supercritical fluid is readily transported through the holes as it has almost zero viscosity. However, the technique relies on heating up sea water to the supercritical temperature, which is 373° C. Heating up water to this temperature requires an amount of heat governed by the heat capacity of water and the latent heat of vapourisation:

$$H = mC\Delta T + mL \quad \text{(A 13)}$$

where H is the heat added to the water, m is the mass of water, C is the specific heat capacity, ΔT is the change in temperature that must occur for the ambient sea water to reach the supercritical temperature and L is the latent heat of vaporisation for water. To continuously heat water to its supercritical point requires the heat to continuously be applied at a power, P_w.

$$P_w = Q\rho_w C\Delta T + Q\rho_w L \quad \text{(A 14)}$$

$$\cong 4\times10^9 Q \quad \text{(A 15)}$$

where P_w is the power that must be applied to heat the water at a rate that can meet the required flow of spray into the atmosphere, Q (m^3 s^{-1}) and ρ_w is the density of the water. We find therefore that, for the supercritical fluid method, the mass of sea water sprayed is proportional to the power required by the sprayers.

B. Flow of water

Sea water must be pumped at a flow rate that depends on several variables. If we assume that the area of the globe to be geoengineered is $A\sim1\times10^{14}$ m^2 (20 % of Earth's surface) and the depth of the boundary layer into which the aerosols are sprayed is $H\sim1000$ m we can calculate the total mass of salt, M, that must be sprayed from the salt mass mixing ratio, q_{salt}:

$$M = (q_{salt})\,A\times H\rho_a \quad \text{(A 10)}$$

where $\rho_a\sim1.2$ kg m^{-3} is the density of air. The aerosol have a life time of around $\tau = 3$ days in the boundary layer (Latham *et al.*, 2008) so we can calculate the flux of salt by dividing Equation A

10 by τ and by dividing by the salinity of sea water, $S=35$ kg m^{-3}, we arrive at the result that the volumetric flux of sea water (m^3 s^{-1}) is proportional to the mass mixing ratio of salt that we require to be present:

$$Q = \frac{(q_{salt})\, AH\rho_a}{S\tau} \tag{A 11}$$

Acknowledgment

...

References

Abdul-Razzak, H., and S. J. Ghan (2000), A parameterization of aerosol activation, part ii: Multiple aerosol types, *J. Geophys. Res.*, *105*.

Abdul-Razzak, H., S. J. Ghan, and C. Rivera-Carpio (1998), A parameterization of aerosol activation. 1. single aerosol type, *J. Geophys. Res.*, *103*, 6123–6131.

Albrecht, B. A. (1989), Aerosols, cloud microphysics and fractional cloudiness, *Science*, *245*, 1227–1230.

Allen, G., H. Coe, A. J. M. Clarke, C. S. Bretherton, R. Wood, S. J. Abel, P. Barrett, P. R. A. Brown, R. George, S. Freitag, C. McNaughton, S. Howell, L. Shank, V. Kapustin, V. Brekhovskikh, L. Kleinman, Y. N. Lee, S. Springston, T. Toniazzo, R. Krejci, J. Fochesatto, G. Shaw, P. Krecl, B. Brooks, P. J. Connolly, J. D. Allan, D. Covert, A. R. Bandy, L. M. Russell, J. Trembath, M. Bart, J. B. McQuaid, J. Wang, and D. Chand (2011), South east pacific atmospheric composition and variability sampled along 20 degrees s during vocals-rex, *Atmos. Chem. & Phys.*, *11*, 5237–5262.

Alterskjaer, K., and J. E. Kristjánsson (2013), The sign of the radiative forcing from marine cloud brightening depends on both particle size and injection amount, *Geophys. Res. Lett.*, *40*, 10.1002/grl.50,117.

Bender, F. A.-M., R. J. Charlson, A. M. L. Ekman, and L. V. Leahy (2011), Quantification of monthly mean regional-scale albedo of marine stratiform clouds in satellite observations and gcms, *J. App. Met. & Climatology*, *50*, 2139–2148.

Bower, K. N., T. W. Choularton, J. Latham, J. Sahraei, and S. Salter (2006), Computational assessment of a proposed technique for global warming mitigation via albedo-enhancement of marine stratocumulus clouds, *Atmos. Res.*, *82*, 328–336.

Connolly, P. J., C. Emersic, and P. R. Field (2012), A laboratory investigation into the aggregation efficiency of small ice crystals, *Atmos. Chem. & Phys.*, *12*, 2055–2076.

Cooper, G., D. Johnston, J. Foster, L. Galbraith, A. Neukermans, B. Ormond, J. Rush, and Q. Wang (2013), A review of some experimental methods for marine cloud brightening, *International Journal of Geosciences*, *4*, 78–97.

Fountoukis, C., and A. Nenes (2005), Continued development of a cloud droplet formation parameterization for global climate models, *J. Geophys. Res.*, *110*, doi:10.1029/2004JD005,591.

Jones, A., J. Haywood, and O. Boucher (2010), A comparison of the climate impacts of geoengineering by stratospheric so2 injection and by brightening of marine stratocumulus clouds, *Atmos. Sci. Lett.*, *10.1002/asl.291*.

Latham, J. (1990), Control of global warming?, *Nature*, *347*, 339–340.

Latham, J. (2002), Amelioration of global warming by controlled enhancement of the albedo and longevity of low-level maritime clouds., *Atmos. Sci. Lett.*, *doi:10.1006/Asle.2002.0048*.

Latham, J., P. Rasch, C.-C. Chen, L. Kettles, A. M. Gadian, A. Gettelman, H. Morrison, K. N. Bower, and T. W. Choularton (2008), Global temperature stabilization via controlled albedo enhancement of low-level maritime clouds, *Phil. Trans. R. Soc. A*, *366*, 3969–3987.

Latham, J., K. N. Bower, T. W. Choularton, H. Coe, P. J. Connolly, G. Cooper, T. Craft, J. Foster, A. M. Gadian, L. Galbraith, H. Iacovides, D. Johnston, B. Launder, B. Leslie, J. Meyer, A. Neukermans, B. Ormond, B. Parkes, P. Rasch, J. Rush, S. Salter, T. Stevenson, H. Wang, Q. Wang, and R. Wood (2012), Marine cloud brightening, *Phil. Trans. R. Soc. A*, *370*, 4217–4262.

Neukermans, A., G. Cooper, J. Foster, L. Galbraith, S. Jain, and B. Ormond (2013), Sub-micrometer salt aerosol production: Marine cloud brightening, in *IEEE Global Humanitarian Technology Conference*, pp. 512–515, San Jose, CA.

Rayleigh, L. (1878), On the instability of jets, *Proc. Lond. Math. Soc.*, *S1-10*, 4–13.

Salter, S., G. Sortino, and J. Latham (2008), Sea-going hardware for the cloud albedo method of reversing global warming, *Phil. Trans. R. Soc. A*, *366*, 3989–4006.

Salter, S., T. Stevenson, and A. Tsiamis (2014), Engineering ideas for brighter clouds, *Issues in environmental science and technology*, *38*, 131–161.

Seinfeld, J. H., and S. N. Pandis (2006), *Atmospheric chemistry and physics: from air pollution to climate change*, 2nd ed., Wiley.

Simpson, E., P. J. Connolly, and G. B. McFiggans (2014), An investigation into the performance of three cloud droplet activation parameterisations, *Geophys. Model. Dev. Discuss.*, *7*, 13–17–1336.

Taylor, G. (1964), Disintegration of water drops in an electric field, *Proc. R. Soc. London.*, *280*, 383–397.

Twomey, S. (1977), The influence of pollution on the shortwave albedo of clouds, *J. Atmos. Sci.*, *34*, 1149–1152.